Superconductivity in Pseudo-Binary Silicide $SrNi_xSi_{2-x}$ with AlB_2-Type Structure

Sunseng PYON[1,2*], Kazutaka KUDO[1,2], and Minoru NOHARA[1,2]

[1] *Department of Physics, Faculty of Science, Okayama University, Okayama 700-8530, Japan*

[2] *Transformative Research-Project on Iron Pnictides (TRIP), Japan Science and Technology Agency (JST), 5 Sanbancho, Chiyoda-ku, Tokyo 102-0075, Japan*

We demonstrate the emergence of superconductivity in pseudo-binary silicide $SrNi_xSi_{2-x}$. The compound exhibits a structural phase transition from the cubic $SrSi_2$-type structure ($P4_132$) to the hexagonal AlB_2-type structure ($P6/mmm$) upon substituting Ni for Si at approximately $x = 0.1$. The hexagonal structure is stabilized in the range of $0.1 < x < 0.7$. The superconducting phase appears in the vicinity of the structural phase boundary. Ni acts as a nonmagnetic dopant, as confirmed by the Pauli paramagnetic behavior.

KEYWORDS: superconductivity, alkaline-earth disilicide, $SrSi_2$, AlB_2-type structure

Alkaline-earth disilicides $AESi_2$ (AE = Ca, Sr, or Ba) exhibit a rich polymorphism owing to their lattice instabilities. Six polymorphic forms have been identified in $AESi_2$: orthorhombic $BaSi_2$-type ($Pnma$), cubic $SrSi_2$-type ($P4_132$), trigonal $EuGe_2$-type ($P\bar{3}m1$), tetragonal α-$ThSi_2$-type ($I4_1/amd$), trigonal $CaSi_2$-type ($R\bar{3}m1$), and hexagonal AlB_2-type ($P6/mmm$).[1–5] Binary $SrSi_2$ shows dimorphism, with a cubic $SrSi_2$-type and a tetragonal α-$ThSi_2$-type. The cubic structure transforms into the tetragonal one under hydrostatic pressures or at elevated temperatures.[2] Cubic $SrSi_2$ is a narrow-gap semiconductor,[6,7] whereas tetragonal $SrSi_2$ is a metal and exhibits superconductivity below 3.1 K.[8] Interestingly, the hexagonal AlB_2-type structure can be stabilized when foreign elements, such as Al and Ga, are partially substituted for Si in $SrSi_2$. Examples are the pseudo-binary compounds $Sr(Al,Si)_2$[9,10] and $Sr(Ga,Si)_2$,[11,12] which crystallize into the AlB_2-type hexagonal structure. These compounds exhibit superconductivity at a superconducting transition temperature of $T_c = 4.7$ and 5.1 K,

*E-mail: pyon@science.okayama-u.ac.jp

respectively. It is widely believed that lattice instabilities often lead to high-T_c superconductivity. The $AESi_2$ system can be a candidate for exploring higher T_c values because their rich polymorphism suggests the presence of strong lattice instabilities.[9–18]

In this Letter, we report superconductivity in pseudo-binary silicide $SrNi_xSi_{2-x}$ with the AlB_2-type structure. When Ni is partially substituted for Si in $SrSi_2$, the structure changes from the cubic $SrSi_2$-type structure into the hexagonal AlB_2-type structure.[19] We demonstrate that the hexagonal structure is stable over a wide range of $0.1 < x < 0.7$ in $SrNi_xSi_{2-x}$. The system exhibits Pauli paramagnetic behavior even though magnetic element Ni is substituted. Furthermore, superconductivity appears at the cubic-hexagonal phase boundary.

Polycrystalline $SrNi_xSi_{2-x}$ samples were prepared by arc-melting. Mixtures with a Sr:Ni:Si ratio of $1{:}x{:}(2-x)$ (where $x = 0.1$, 0.2, 0.3, 0.4, 0.5, 0.6, 0.7, 0.8, and 1.0) were pelletized and melted in an Ar atmosphere using an arc furnace. The structure of the samples was examined by powder X-ray diffraction (XRD) measurements. Magnetization was measured using a SQUID magnetometer (Quantum Design MPMS). Electrical resistivity was measured by a standard DC four-terminal method using a Quantum Design PPMS. Specific heat was measured by a relaxation method using a PPMS.

XRD measurements clarified that a single phase of polycrystalline samples was successfully synthesized for $x = 0.2$, 0.3, 0.4, 0.5, and 0.6. In the case of $x = 0.1$, the cubic phase (the $SrSi_2$-type structure) was obtained with a small amount of the hexagonal phase (the AlB_2-type structure). The $x = 0.7$ sample was a mixture of the hexagonal phase and impurity phase(s). The hexagonal phase was not obtained for $x \geq 0.8$, suggesting a solubility limit at approximately $x = 0.7$. Lattice parameters a and c in the hexagonal phase at $0.1 \leq x \leq 0.7$, determined by XRD analysis, are shown in Fig. 1(a) as a function of x. The a parameter increases and the c parameter decreases with increasing Ni content x. The monotonic behavior of the lattice parameters suggests that a solid solution of $SrNi_xSi_{2-x}$ was successfully obtained in the hexagonal phase. The evolution of the crystal structures as a function of x is summarized in Fig. 1(b). The structural phase boundary between the cubic and hexagonal phases exists at approximately $x = 0.1$. The hexagonal structure in $SrNi_xSi_{2-x}$ is stabilized in the range $0.1 < x < 0.7$. The solubility limit is located at $x \simeq 0.7$.

In this system, $SrNi_xSi_{2-x}$, a superconducting phase emerges in a narrow Ni-doping range near the cubic-hexagonal boundary at the hexagonal side, as shown in Fig. 1(b). This is illustrated by the low-temperature resistivity ρ and the magnetization M data

shown in Figs. 2(a) and 2(b), respectively. For $x = 0.1$, 0.2, and 0.3, zero resistivities and diamagnetic signals, a hallmark of superconductivity, were detected below $T_c = 2.3$, 2.6, and 2.8 K, respectively. The shielding volume fractions were 119% and 106% for the $x = 0.2$ and 0.3 samples, respectively. The shielding volume fraction was significantly lower for the $x = 0.1$ sample, because this sample is dominated by the nonsuperconducting cubic phase; the superconductivity at $T_c = 2.3$ K can be ascribed to the hexagonal phase at $x = 0.1$. Bulk superconductivity was not detected for the $x = 0.4$, 0.5, 0.6, or 0.7 sample. Although the $x = 0.4$ sample showed zero resistivity, a negligibly small diamagnetic signal (with a shielding volume fraction lower than 0.1% at 1.8 K) suggests that the superconducting phase was not a bulk one for $x = 0.4$. For the $x = 0.5$, 0.6 and 0.7 samples, neither zero resistivity nor diamagnetic behavior was observed above 1.8 K.

For further understanding of the superconducting state in $SrNi_xSi_{2-x}$, we performed resistivity measurements in applied magnetic fields to determine the upper critical field H_{c2} of the $x = 0.3$ sample, at which the highest T_c was observed. Figure 3(a) shows the temperature dependence of H_{c2}, which was determined from the midpoint of the resistive transition, shown in Fig. 3(b). The extrapolation to 0 K using the Werthamer-Helfand-Hohenberg (WHH) theory[20] gives an estimate for the $H_{c2}(0)$ value of 1.58 T. The $H_{c2}(0)$ value was roughly similar to that of a pseudo-binary alkaline-earth silicide $Ca(Al,Si)_2$ with an AlB_2-type structure.[21,22] We estimated the coherence length to be $\xi_0 = (\Phi_0/[2\pi H_{c2}(0)])^{1/2} = 144$ Å, where Φ_0 is the magnetic flux quantum. The Pauli limiting field $H_{\rm Pauli} = 1.84T_c = 5.2$ T was larger than the estimated H_{c2}. These results demonstrate that $SrNi_xSi_{2-x}$ is a conventional type-II superconductor.

To understand the role of Ni, we compared the normal-state resistivity of the superconducting sample ($x = 0.2$) with that of the nonsuperconducting sample ($x = 0.6$). Figure 4(a) shows ρ as a function of temperature from 2 to 300 K for the $x = 0.2$ and 0.6 samples. ρ exhibits an almost temperature-independent behavior above $T_c = 2.6$ K for $x = 0.2$, suggesting that the sample is a bad metal. In contrast to that, ρ for $x = 0.6$ shows a noticeable metallic behavior with a positive temperature coefficient. Another noticeable feature is the reduction of the residual resistivity for the $x = 0.6$ sample. We naively expect that disorder increases with Ni doping x, resulting in an increase in the residual resistivity. However, what we observed was a decrease in the residual resistivity with x. Thus, the observed reduction of the residual resistivity suggests an increase in carrier concentration with Ni doping. In other words, Ni acts to dope charge carriers in

$SrNi_xSi_{2-x}$.

Magnetic susceptibility as a function of temperature is shown in Fig. 4(b) for the superconducting and the nonsuperconducting samples from 10 to 300 K. The data show almost temperature-independent Pauli paramagnetic behaviors. This behavior is characteristic of metals and is consistent with the (metallic) behavior of the resistivity. By assuming the core diamagnetism of Sr^{2+} to be -20×10^{-6} emu/mol, we estimate the Pauli paramagnetic susceptibility to be $\chi_{\rm Pauli} \simeq 25\times10^{-6}$ and $\simeq 50\times10^{-6}$ emu/mol for $x = 0.2$ and 0.6, respectively. These values are quite small and are comparable with those of *sp* metals, suggesting that the electronic density of state at the Fermi level is small and the contribution of Ni 3*d* orbitals is negligible even for the heavily Ni-doped sample ($x = 0.6$). This is consistent with the small electronic specific-heat coefficient γ $\simeq 3.8$ mJ/molK^2 (for $x = 0.3$), as we describe in the following.

The superconducting transition temperature T_c increases monotonously with Ni doping at $0.1 \le x \le 0.3$ in $SrNi_xSi_{2-x}$. Intriguingly, the superconducting phase disappears suddenly at approximately $x = 0.35$, as shown in Fig. 1(b). This non-monotonous dependence of T_c on doping x accords with the electronic density of states (DOS) at the Fermi level, and thus with the electronic specific-heat coefficient γ. We determined γ from the specific heat C using the C/T-versus-T^2 plot in Fig. 5, and plotted γ as a function of x in Fig. 1(c). γ increases with x in the superconducting region ($0.1 < x \le 0.3$), at which T_c increases with x. γ suddenly decreases at $x \simeq 0.4$, above which superconductivity disappears. Such non-monotonous changes of T_c on doping have been reported on $CaAl_{2-x}Si_x$[9] and $SrGa_xSi_{2-x}$.[12] Contrary to the decrease in the specific-heat coefficient γ at $x \simeq 0.4$, the value of Pauli paramagnetic susceptibility increases; $\chi_{\rm Pauli} \simeq 25\times10^{-6}$ emu/mol for the superconducting region, while $\chi_{\rm Pauli} \sim 50\times10^{-6}$ emu/mol for the nonsuperconducting region at $x \ge 0.4$, as can be seen from Fig. 4(b). We do not understand the reason for this at present. Further studies are invaluable.

Specific heat shows a clear jump at T_c, indicative of bulk superconductivity, for $x = 0.2$ and 0.3, as shown in Fig. 5. We estimate the ratio of specific-heat jump at T_c to γT_c to be $\Delta C(T_c)/\gamma T_c \simeq 0.8$, using $\gamma = 3.8$ mJ/molK^2 and $\Delta C(T_c)/T_c = 3.2$ mJ/molK^2 for $x = 0.3$. The ratio is smaller than 1.43, the value of the BCS weak coupling limit. We ascribe this to the presence of a residual normal-state region, likely due to the inhomogeneity of the samples.

Two intriguing features emerged from this study. First, Ni acts as a nonmagnetic dopant; superconductivity emerged by substituting Ni for Si in $SrNi_xSi_{2-x}$. In gen-

eral, magnetic elements are harmful for superconductivity because of severe magnetic pair breaking. In contrast to this fate, the magnetic element Ni acts as a nonmagnetic dopant without inducing any local magnetic moments in hexagonal $SrNi_xSi_{2-x}$ in the entire x range of $0.1 < x < 0.7$. We naively expect that Ni $3d$ orbitals are completely filled in $SrNi_xSi_{2-x}$, as inferred from the small Pauli susceptibility. This finding suggests that magnetic elements can be utilized as a dopant for producing superconductivity. Second, the superconductivity of $SrNi_xSi_{2-x}$ emerged at the critical vicinity of the cubic-hexagonal phase boundary. This result suggests that the structural instabilities play an important role in the occurrence of superconductivity in $SrNi_xSi_{2-x}$. A similar phenomenon is known in $Ba_{1-x}K_xBiO_3$, in which superconductivity at up to T_c = 32 K appears in the vicinity of the cubic and orthorhombic phase boundary.[23–25] The mechanism of superconductivity in $Ba_{1-x}K_xBiO_3$ is still in debate, though the importance of structural instabilities for describing the physical properties of $Ba_{1-x}K_xBiO_3$, including the origin of the superconductivity, is recognized.[26] The analogy between the two systems suggests the importance of lattice instabilities in the occurrence of the superconductivity in $SrNi_xSi_{2-x}$.

In summary, pseudo-binary silicides $SrNi_xSi_{2-x}$ were synthesized by arc-melting, and their magnetic and electrical properties were characterized. It was demonstrated that the semiconducting phase with a cubic $SrSi_2$-type structure changes into a metallic phase with a hexagonal AlB_2-type structure upon partial substitution of Ni for Si in $SrSi_2$; the hexagonal phase is stabilized at $0.1 < x < 0.7$ in $SrNi_xSi_{2-x}$; superconductivity at up to 2.8 K appears at $0.1 \leq x \leq 0.3$. The system showed a Pauli paramagnetic behavior, although the magnetic element Ni was substituted for Si. Superconductivity, which was a conventional type-II type, emerged in the critical vicinity of the cubic-hexagonal phase boundary.

Acknowledgment

We are indebted to Y. Ikeda, S. Araki, and T. C. Kobayashi for their help in using the arc furnace. This work was partially performed at the Advanced Science Research Center, Okayama University. It was partially supported by Grants-in-Aids for Scientific Research from the Japan Society for the Promotion of Science (JSPS) and the Ministry of Education, Culture, Sports, Science, and Technology (MEXT), Japan.

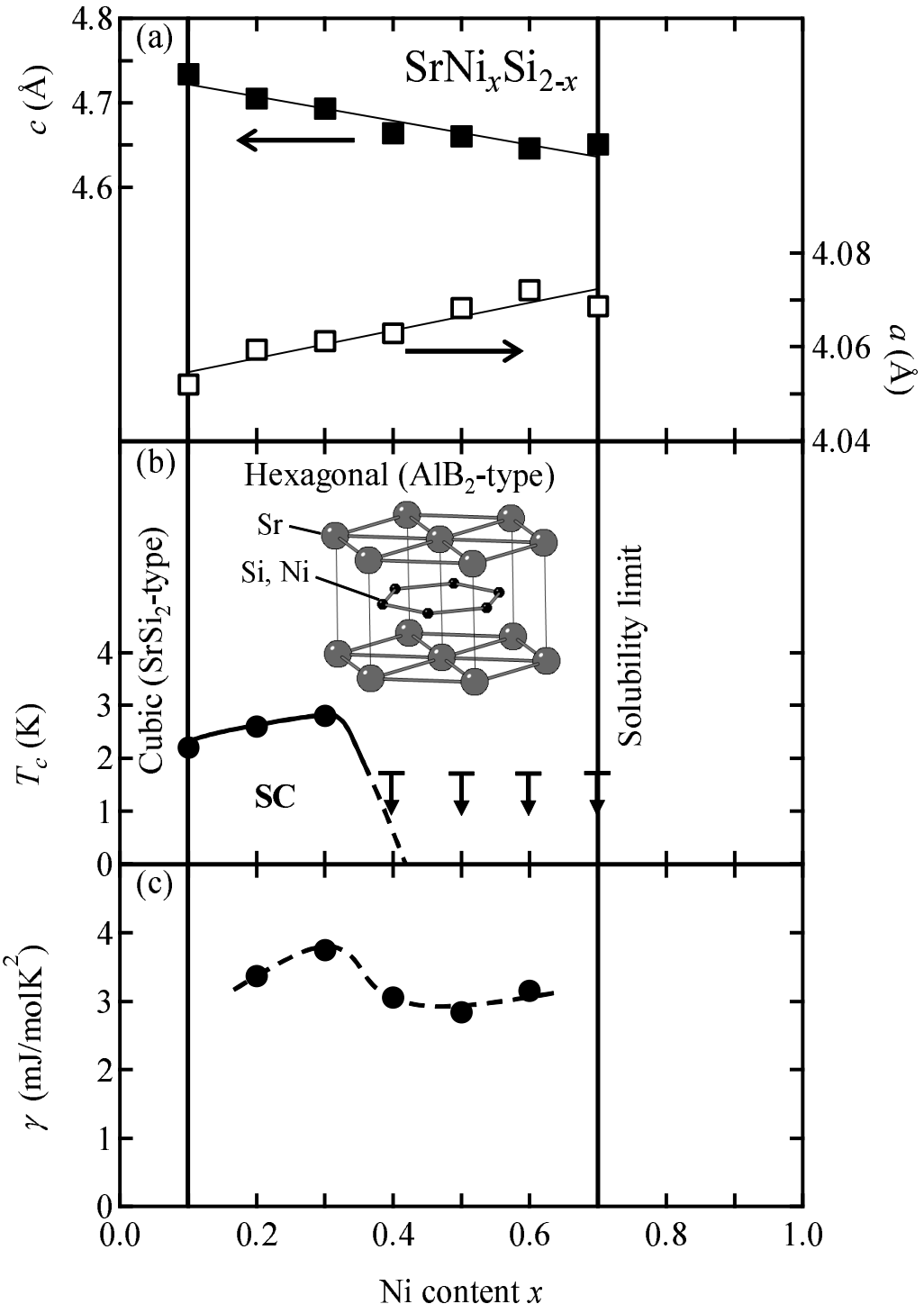

Fig. 1. (a) Lattice parameters, determined from XRD measurements, in the hexagonal lattice at room temperature as functions of x for $SrNi_xSi_{2-x}$. (b) Structural and superconducting phase diagram of $SrNi_xSi_{2-x}$. Closed circles indicate superconducting transition temperatures T_c determined from magnetization measurements. Bars and arrows indicate the absence of bulk superconductivity above 1.8 K. The inset schematically illustrates the crystal structure of hexagonal AlB_2-type $SrNi_xSi_{2-x}$. (c) Electronic specific-heat coefficient γ as a function of x for $SrNi_xSi_{2-x}$, which was estimated from linear extrapolation of the C/T-versus-T^2 data in the normal state.

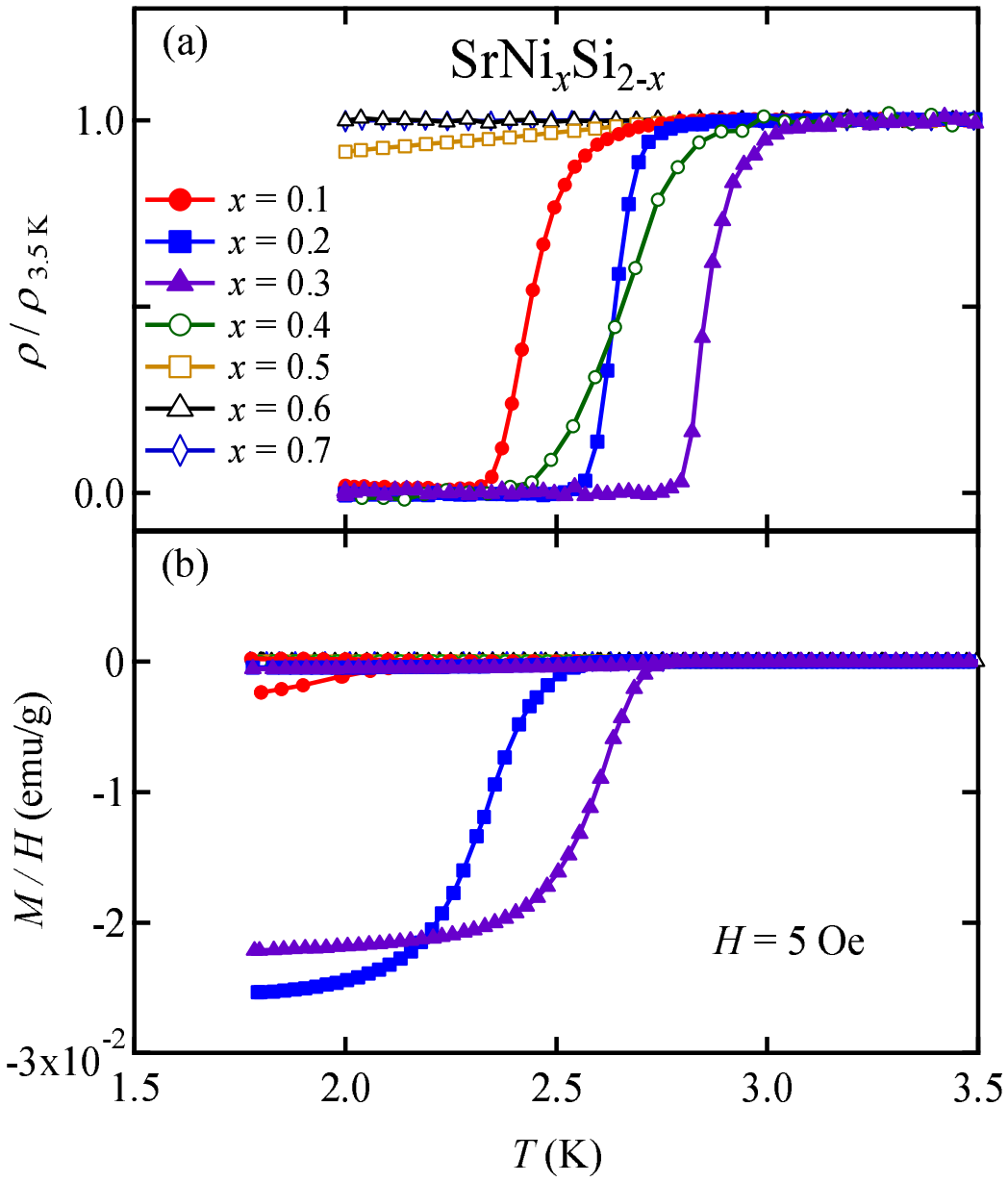

Fig. 2. (Color online) (a) Low-temperature resistivity of $SrNi_xSi_{2-x}$ (normalized by the value of ρ at $T = 3.5$ K) in zero applied field. (b) Low-temperature magnetization of $SrNi_xSi_{2-x}$. The measurements of magnetization were conducted in an applied field of $H = 5$ Oe with zero-field-cooled and field-cooled processes. The shielding volume fraction for $x = 0.2$ and 0.3 reached 119% and 106%, respectively, at 1.8 K.

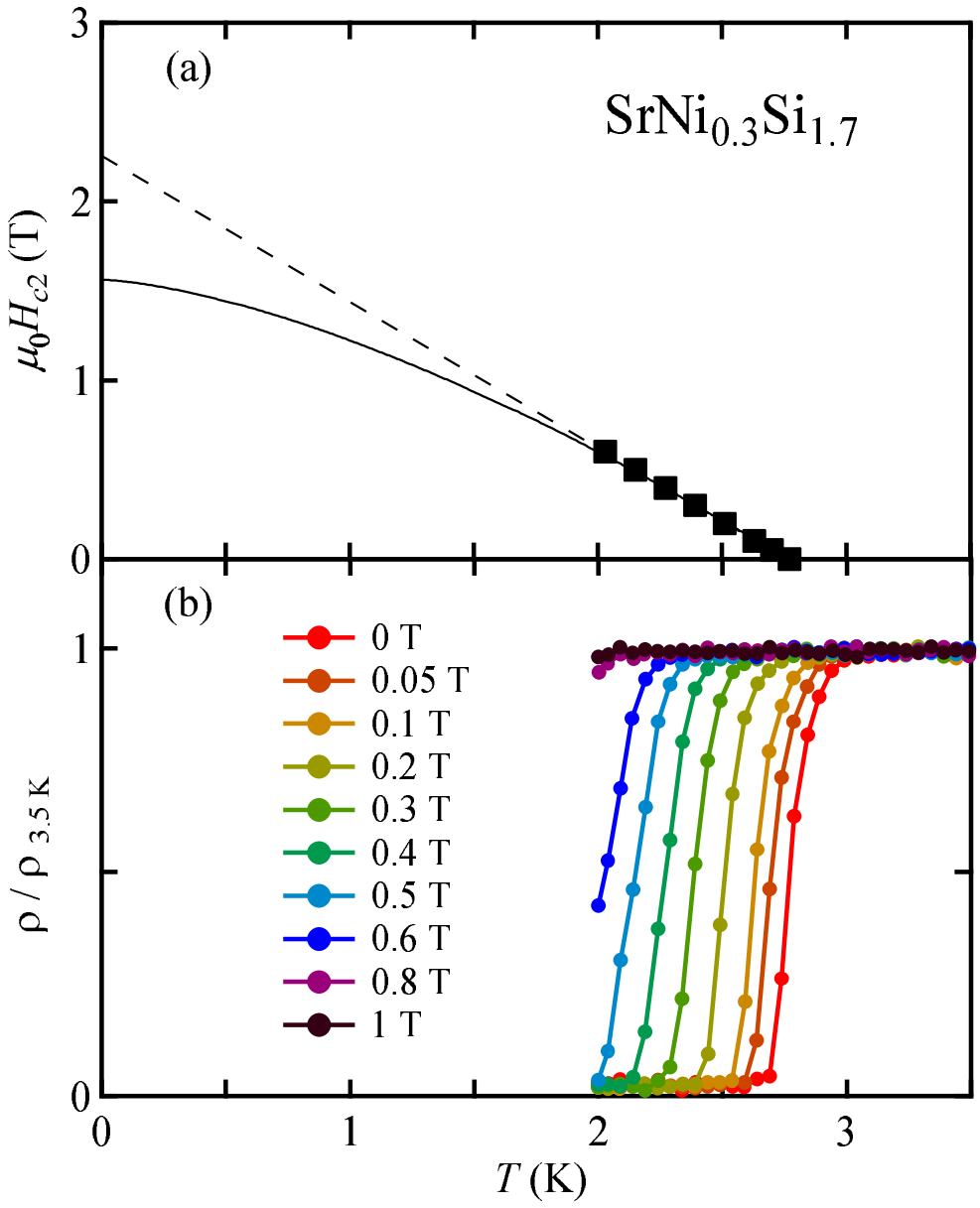

Fig. 3. (Color online) (a) Temperature dependence of the upper critical field H_{c2} for $SrNi_xSi_{2-x}$ with $x = 0.3$. The solid line shows the WHH behavior. The broken line yields a slope of $-dH_{c2}/dT|_{T=T_c} = 0.82$ T/K. (b) Low-temperature resistivity in various applied fields for $SrNi_xSi_{2-x}$ with $x = 0.3$.

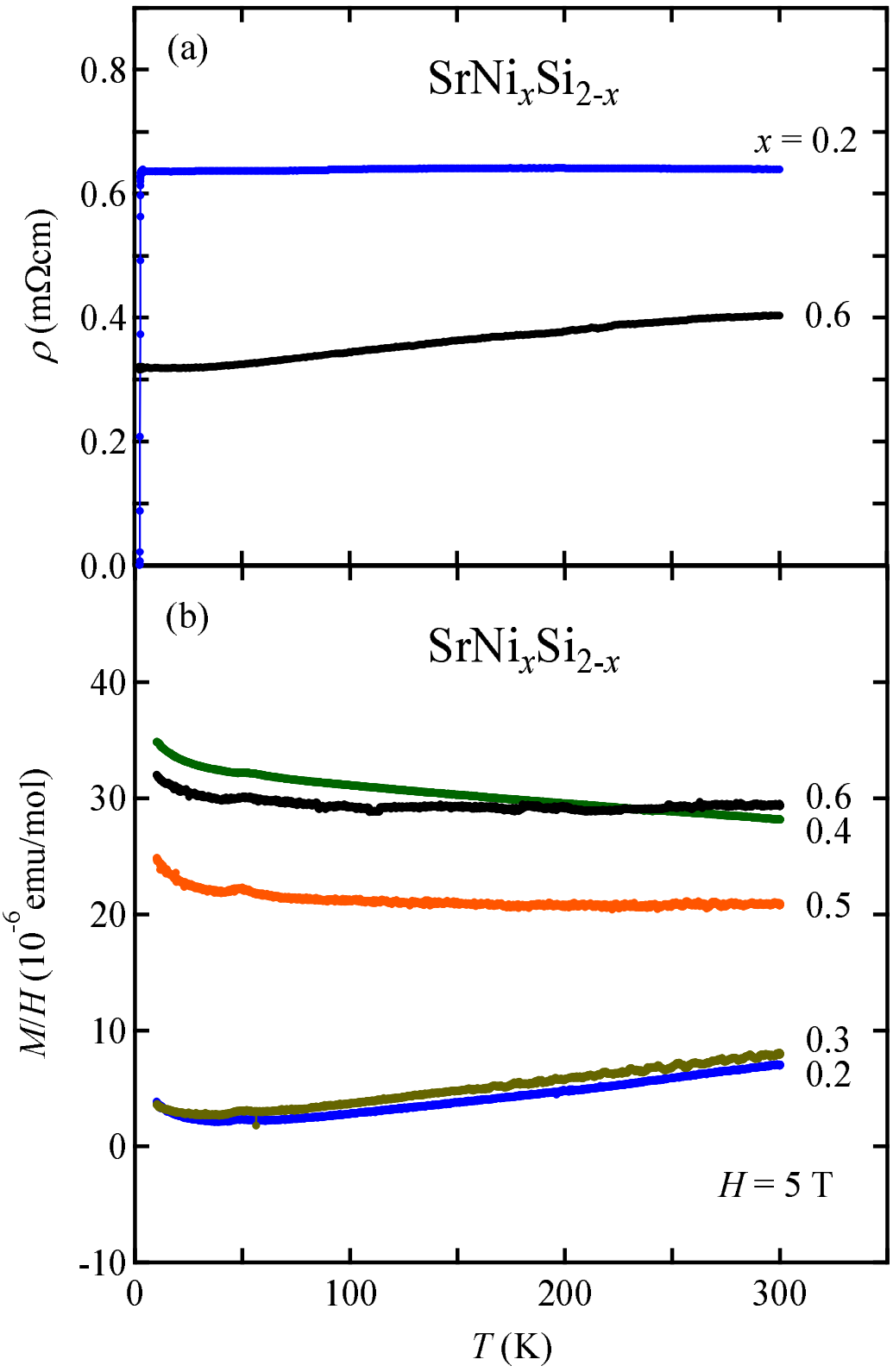

Fig. 4. (Color online) (a) Electrical resistivity ρ of $SrNi_xSi_{2-x}$ for $x = 0.2$ and 0.6, as a function of temperature. (b) Temperature dependence of magnetization M divided by H, M/H, in a magnetic field H of 5 T for $SrNi_xSi_{2-x}$.

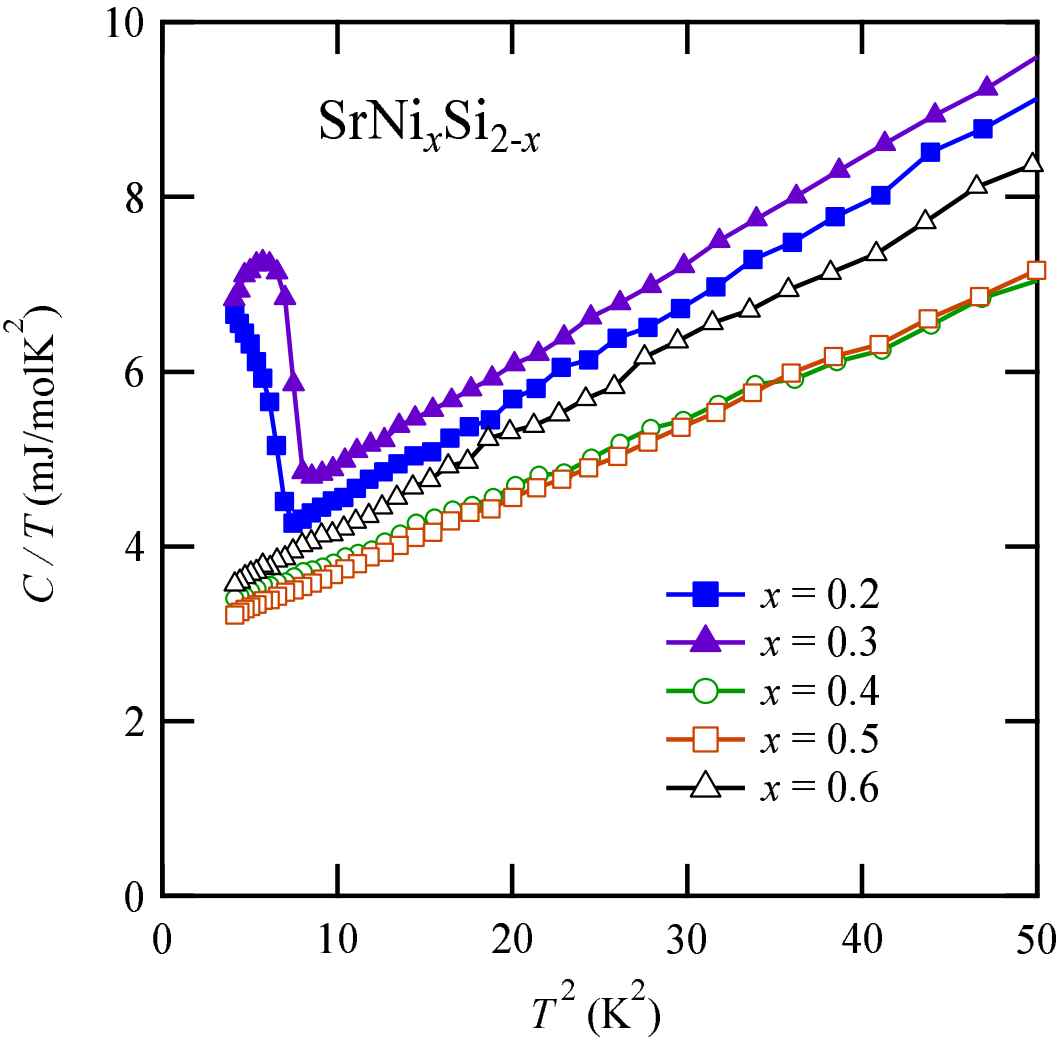

Fig. 5. (Color online) Specific heat divided by temperature, C/T, as a function of T^2 for $SrNi_xSi_{2-x}$ in zero applied field.

References

1) M. Imai, and T. Kikegawa: Chem. Mater. **15** (2003) 2543.

2) J. Evers: J. Phys. Chem. Solids **40** (1979) 951.

3) J. Evers: J. Solid State Chem. **28** (1979) 369.

4) P. Bordet, M. Affronte, S. Sanfilippo, M. Núñez-Regueiro, O. Laborde, G. L. Olcese, A. Palenzona, S. LeFloch, D. Levy, and M. Hanfland: Phys. Rev. B **62** (2000) 11392.

5) J. Evers: J. Solid State Chem. **32** (1980) 77.

6) M. Imai, T. Naka, T. Furubayashi, H. Abe, T. Nakama, and K. Yagasaki: Appl. Phys. Lett. **86** (2005) 032102.

7) D. B. McWhan, V. B. Compton, M. S. Silverman, and J. R. Soulen: J. Less-Common Met. **12** (1967) 75.

8) J. Evers, G. Oehlinger, and H. R. Ott: J. Less-Common Met. **69** (1980) 389.

9) B. Lorenz, J. Lenzi, J. Cmaidalka, R. L. Meng, Y. Y. Sun, Y. Y. Xue, and C. W. Chu: Physica C **383** (2002) 191.

10) M. J. Evans, Y. Wu, V. F. Kranak, N. Newman, A. Reller, F. J. Garcia-Garcia, and U. Häussermann: Phys. Rev. B **80** (2009) 064514.

11) M. Imai, E. Abe, J. Ye, K. Nishida, T. Kimura, K. Honma, H. Abe, and H. Kitazawa: Phys. Rev. Lett. **87** (2001) 077003.

12) R. L. Meng, B. Lorenz, Y. S. Wang, J. Cmaidalka, Y. Y. Sun, Y. Y. Xue, J. K. Meen, and C. W. Chu: Physica C **382** (2002) 113.

13) M. Imai, K. Nishida, T. Kimura, and H. Abe: Appl. Phys. Lett. **80** (2002) 1019.

14) H. H. Sung, and W. H. Lee: Physica C **406** (2004) 15.

15) M. Imai, K. Nishida, T. Kimura, H. Kitazawa, H. Abe, H. Kitô, and K. Yoshii: Physica C **382** (2002) 361.

16) M Imai, K. Nishida, T. Kimura, and H. Abe: Physica C **377** (2002) 96.

17) S. Yamanaka, T. Otsuki, T. Ide, H. Fukuoka, R. Kumashiro, T. Rachi, K. Tanigaki, FZ. Guo, and K. Kobayashi: Physica C **451** (2007) 19.

18) W. J. Hor, H. H. Sung, and W. H. Lee: Physica C **434** (2006) 121.

19) N. Nasir, N. Melnychenko-Koblyuk, A. Grytsiv, P. Rogl, G. Giester, J. Wosik, and G. E. Nauer: J. Solid State Chem. **183** (2010) 565.

20) N. R. Werthamer, E. Helfand, and P. C. Hohenberg: Phys. Rev. **147** (1966) 295.

21) A. K. Ghosh, M. Tokunaga, and T. Tamegai: Phys. Rev. B **68** (2003) 054507.

22) T. Tamegai, A. K. Ghosh, Y. Hiraoka, and M. Tokunaga: Physica C **408-410** (2004) 146.

23) R. J. Cava, B. Batlogg, J. J. Krajewski, R. Farrow, L. W. Rupp Jr, A. E. White, K. Short, W. F. Peck, and T. Kometani: Nature **332** (1988) 814.

24) D. G. Hinks, B. Dabrowski, J. D. Jorgensen, A. W. Mitchell, D. R. Richards, S. Pei, and D. Shi: Nature **333** (1988) 836.

25) S. Pei, J. D. Jorgensen, B. Dabrowski, D. G. Hinks, D. R. Richards, A. W. Mitchell, J. M. Newsam, S. K. Sinha, D. Vaknin, and A. J. Jacobson: Phys. Rev. B **41** (1990) 4126.

26) S. Zherlitsyn, B. Lüthi, V. Gusakov, B. Wolf, F. Ritter, D. Wichert, S. Barilo, S. Shiryaev, C. Escribe-Filippini, and J. L. Tholence: Eur. Phys. J. B **16** (2000) 59.

Note added in proof - We noticed a paper by K. Inoue, K. Kawashima, T. Ishikawa, M. Fukuma, T. Okumura, T. Muranaka, and J. Akimitsu, presented at 24th Int. Symposium on Superconductivity (ISS 2011) on October 26, 2011, reporting similar results.